

Free-Decay Time-Domain Modal Identification for Large Space Structures

Hyoung M. Kim,* David A. VanHorn,† and Harold H. Doiron‡
McDonnell Douglas Aerospace-Space Systems, Houston, Texas 77059

Concept definition studies for the Modal Identification Experiment (MIE), a proposed space flight experiment for the Space Station Freedom, have demonstrated advantages and compatibility of free-decay time-domain modal identification techniques with the on-orbit operational constraints of large space structures. Since practical experience with modal identification using actual free-decay responses of large space structures is very limited, several numerical and test data reduction studies were conducted. Major issues and solutions were addressed, including closely spaced modes, wide frequency range of interest, data acquisition errors, sampling delay, excitation limitations, nonlinearities, and unknown disturbances during free-decay data acquisition. The data processing strategies developed in these studies were applied to numerical simulations of the MIE, test data from a deployable truss, and launch vehicle flight data. Results of these studies indicate free-decay time-domain modal identification methods can provide accurate modal parameters necessary to characterize the structural dynamics of large space structures.

Introduction

IN conventional modal analysis, impulse response functions calculated from inverse Fourier transforms of frequency response functions (FRFs) have been widely used with time-domain modal identification algorithms.^{1,2} This approach is called a forced response technique since the FRF is determined using both input and output measurements from the forced response testing of structures (Fig. 1). Indirect free-decay data obtained in this manner is relatively noise free and absent of significant nonlinearities due to the large number of data averages used to obtain high-quality FRFs. For large space structures,³⁻⁵ a low-frequency range of interest (less than 0.1 Hz) requires longer data records per each average in FRF calculations. In addition, large numbers of excitation points and structural nonlinearities require large numbers of averages. Finally, computational limitations precluded the use of direct forced response techniques, e.g., ARMAX⁶ and OKID⁷ methods, on large space structures such as the Space Station Freedom (SSF). These methods, which use both input (force) and output (response) data without FRF calculation, have been used for identification of small linear systems.

In free-decay modal analysis, the modal identification algorithm is applied directly to free-decay responses of the structure, instead of impulse response functions. This free-decay technique not only significantly reduces the test time for large space structures, but also eliminates the need to measure the input force to the structure (Fig. 1). In addition, changes in modal parameters can be characterized by identifying different linearized models over short periods of the free-decay data rather than using the entire period, which is necessary in a forced response technique.

The modal identification experiment (MIE) is a proposed flight experiment to characterize the structural dynamics of the SSF. The baseline experiment consists of excitation of the SSF, measurement of the structural responses, recording and transmitting the measurement data, and ground-based data processing for modal identification.⁸ In the case of the MIE, a decision was made to conduct excitation and response measurements during the night portion of an orbit (less than 45 min duration) to minimize impacts on

the SSF operations and effects of thermal transients on structural responses. This time constraint severely limits the number of averages in the FRF calculation for forced response testing since the low-frequency range of interest (0.1–2.0 Hz) dictates long sample times.⁹ Attitude control system (ACS) and reboost thrusters of the SSF were found to be the most suitable available excitation sources.¹⁰ Although the applied force from each thruster firing can be estimated by measuring the combustion chamber pressure, it is not practical to directly measure the input force, which is essential

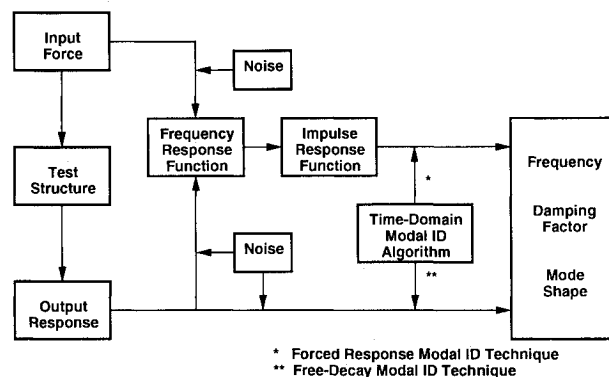
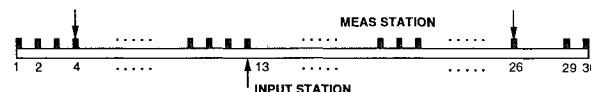


Fig. 1 Free-decay vs. forced response modal identification techniques.



NO	FREQ,HZ	DAMP,%	NO	FREQ,HZ	DAMP,%	SF, %
1	0.100	1.0	2	0.103	1.0	3.0
3	0.150	1.0	4	0.155	1.0	3.3
5	0.350	1.0	6	0.360	1.0	2.9
7	1.50	1.0	8	1.55	1.0	3.3
9	4.00	1.0	10	4.10	1.0	2.5

$$* \text{SEPARATION FACTOR OF CLOSELY SPACED MODES (\%)} = \frac{F_2 - F_1}{F_1} \times 100$$

Fig. 2 10 DOF linear system model.

Presented as Paper 92-2208 at the AIAA/ASME/ASCE/AHS/ASC 33rd Structures, Structural Dynamics, and Materials Conference, Dallas, TX, April 13–15, 1992; received Dec. 8, 1992; revision received July 23, 1993; accepted for publication July 26, 1993. Copyright © 1992 by the American Institute of Aeronautics and Astronautics, Inc. All rights reserved.

*Staff Engineer, Space Station Division. Member AIAA.

†Engineer-Specialist, Space Station Division. Member AIAA.

‡Senior Manager, Space Station Division. Member AIAA.

in calculating FRFs. Thus, the test time and force measurement constraints led to selection of a free-decay time-domain modal identification technique as a baseline for the MIE design.

Although direct free-decay modal identification for the MIE is more compatible with operational constraints of the SSF, there are legitimate concerns about the modal identification performance of this approach due to lack of practical experience.¹¹ In addition, the on-orbit modal identification difficulties presented by large space structures such as the SSF are challenging for even the most highly developed modal testing methods. To address these concerns, several studies were conducted to develop data processing techniques and evaluate free-decay time-domain modal identification performance relative to major issues such as closely spaced modes, wide frequency range of interest, data acquisition errors, sampling delay, excitation limitations, nonlinearities, and unknown disturbances during free-decay data acquisition.

These studies are organized into two main sections of the paper, entitled Free-Decay Modal Identification Methods Development and Case Studies. The eigensystem realization algorithm (ERA) was selected in the study to determine natural frequencies, damping factors, and mode shapes.¹² In the first section, numerical simulations with relatively simple mathematical models are employed to illustrate free-decay testing, and data processing techniques are developed to address modal identification performance concerns. In the Case Studies section, performance of the developed free-decay modal identification techniques is presented through numerical simulations of the MIE and compared to a burst random FRF modal identification alternative approach for the MIE. Also, results of free-decay modal identification using ground test data of a deployable truss and flight data of a launch vehicle are presented.

Free-Decay Modal Identification Methods Development

Closely Spaced Modes, High Frequency Aspect Ratio, and Sampling Delay

A 10 degrees of freedom (DOF) linear system model (Fig. 2) was created to investigate the problems of closely spaced modes, high frequency aspect ratio, and sampling delay. The frequency aspect ratio is defined as the ratio of the highest target frequency to the lowest target frequency. Although this model does not represent any particular physical system, it allows one to arbitrarily select frequency, damping factor, and mode shape for parametric studies. Thirty accelerometer locations were simulated along the length and response data was sampled at 50 Hz. It is noted that response data from 10 of 30 measuring stations are linearly independent. Data acquisition errors due to electrical random noise from the accelerometer, signal conditioning electronics, and electromagnetic interference were added to the simulated response data. The model contained five sets of closely spaced modes (separation factors were about 3%) and a frequency aspect ratio of 40 (from 0.1 to 4.0 Hz). The separation factor for closely spaced modes is defined as the frequency difference as a percent of the lower mode frequency; for instance, the separation factor of repeated modes is zero.

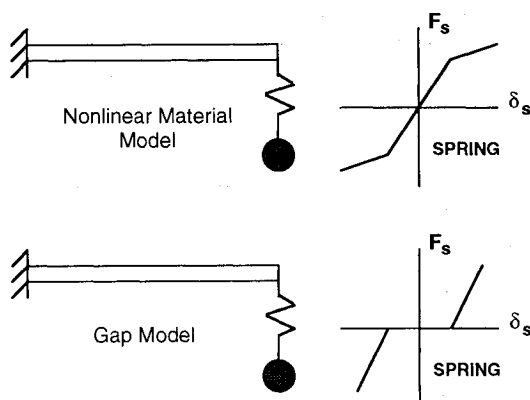


Fig. 3 Nonlinear material and gap models.

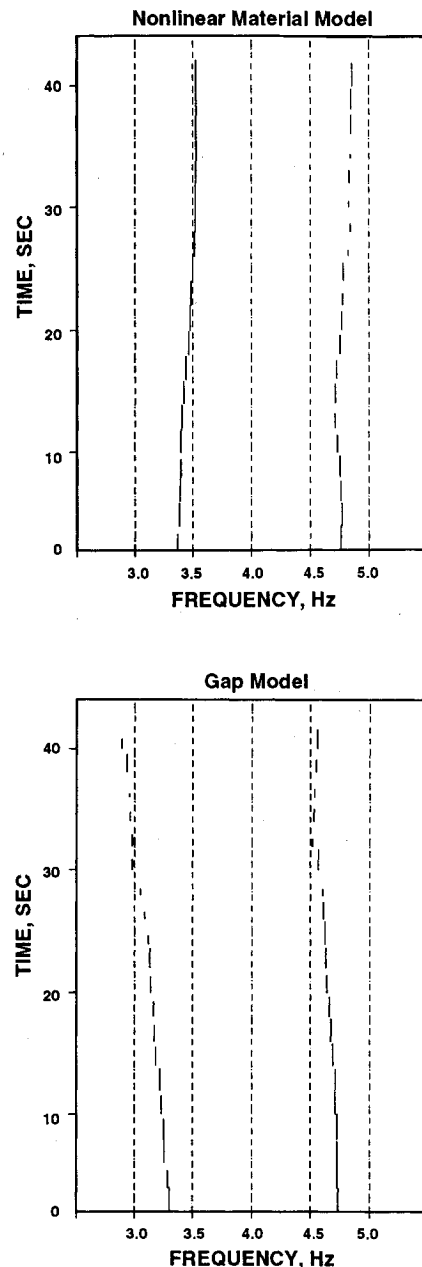


Fig. 4 Frequency time history for nonlinear models.

Repeated modes are not identifiable from the response with a single input or a single initial condition for the free-decay response. Theoretically, there must be the same number of linearly independent initial conditions as the number of repeated modes at a frequency. Closely spaced modes, though theoretically possible to identify with a single initial condition, can cause similar problems in practice due to numerical instability and measurement noise. This problem can be solved by employing multi-initial condition modal identification, where the number of initial conditions should be, at least, the number of modes in the modal cluster. In the simulation, only 6 of the 10 modes were indicated by the frequency spectrum due to the presence of closely spaced modes. With a single initial condition (equivalent to a single-point input for the forced response modal identification method), identification of all 10 modes failed. By using three linearly independent data sets produced by placing the impulse force at different locations, all 10 modes were clearly identified.

A large frequency aspect ratio can also preclude the identification of all modes through one run of the modal identification algorithm. The main problem is the large variation in the number of cycles for each mode in the fixed-time-length data record. For

example, if a 4-s data record was sampled at 25 Hz (100 data samples), the system identified by ERA would emphasize the higher frequency modes since the data contain 16 cycles of a 4.0-Hz mode, but less than a half-cycle of data for a 0.1-Hz mode. On the other hand, if a 20-s data record was sampled at 5 Hz (100 data samples), the algorithm would emphasize the lower frequency modes with aliasing effects on the higher frequency modes.

The use of multiple ERA runs with different frequency ranges can solve this problem, which is similar to a zooming technique in the frequency domain. The entire frequency range is subdivided into a series of shorter frequency ranges. Within each frequency range, a different sampling frequency is used and a band-pass finite impulse response (FIR) filter is applied to eliminate aliasing effects. This approach is called a time-domain zooming technique. In the simulation, three ERA modal identification runs were made for frequency ranges of 0.0–1.0 Hz, 1.0–3.0 Hz, and 3.0–5.0 Hz. Parameters within ERA were manipulated to give equivalent sampling frequencies of 5, 10, and 25 Hz, respectively. All 10 modes were identified with a maximum frequency error of 0.1%.

Sampling delay is a form of data acquisition error that occurs when all measurement channels are not sampled simultaneously. This can result in erroneous modal parameters, especially mode shapes. For example, the current data acquisition system design for the MIE may allow a maximum of 1 ms delay between multiplexer/demultiplexers (MDM) and a cumulative 50- to 130- μ s delay between channels within the same MDM.

Response data from the linear system model was modified so that there were three MDMs and each MDM handled 10 measurement channels. Sampling delay between the MDMs was simulated by

$$T_m = 1 \text{ ms} \times \text{random}(0, 1) \quad (1)$$

and the sampling delay between channels was assumed to be

$$T_c = 50 \mu\text{s} + 80 \mu\text{s} \times \text{random}(0, 1) \quad (2)$$

The total sampling delay of each channel was estimated by

$$\text{Sampling Delay} = T_m + \sum_{i=1}^c T_{ci} \quad (3)$$

The ERA identified the exact natural frequencies and mode shapes, but had a maximum error of 6% in the damping factors. It is noted that the major portion of the sampling delay for the MIE can be compensated from the MDM data, if necessary.

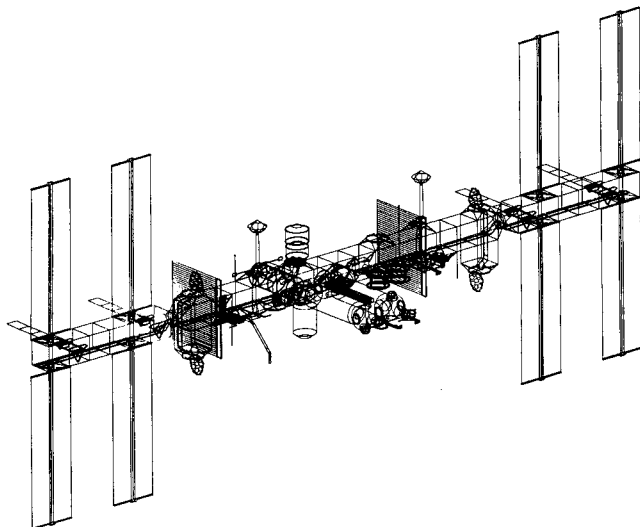


Fig. 5 Space Station Freedom: assembly complete configuration.

Table 1 MIE modal identification results

Modal ID method	No. of data record	Modal damping (%)	No. of identified modes	
			No noise	Noise
Free-decay	4	1	— ^a	20
	4	2	15	13
Forced response	8	2	12	1
	12	2	17	4
	16	2	18	8

^aNot included in the study.

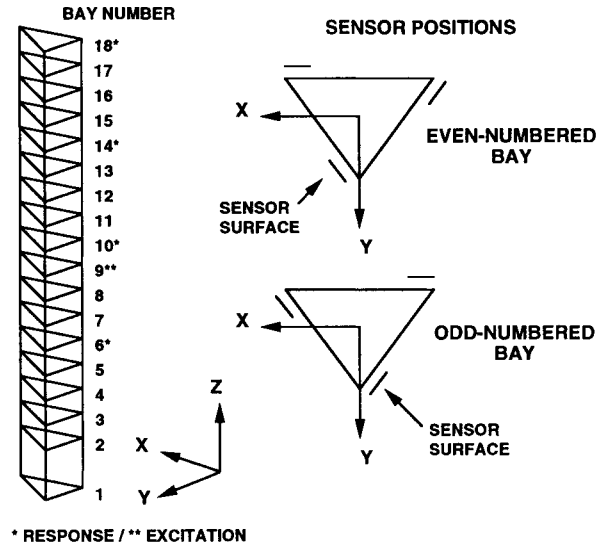


Fig. 6 Mini-Mast deployable truss.

Nonlinearities

Most modal identification algorithms assume that the test structure is linear. Although there are several techniques available for nonlinear systems, it will be difficult to characterize the nonlinearities in large and complex structures such as the SSF by on-orbit modal testing. The forced response modal identification method utilizing FRFs can identify a linearized model if the test structure behaves within a reasonable linear range during the entire test period. However, a free-decay time domain modal identification technique assumes linear behavior during a relatively short time period. By identifying different linearized models over short periods of the free-decay data records, changes in nonlinear behavior of modal parameters can be identified with respect to different levels of the responses. This approach is called a sliding time window technique.¹³

There are three types of nonlinearities common to most structures including material nonlinearity, nonlinearity due to loose joints, and geometric nonlinearity. The first two nonlinearities were incorporated into a linear cantilever beam model to evaluate the ability of the free-decay time-domain technique to assess nonlinearity (Fig. 3). The linear cantilever beam has a lumped mass that is about 5% of the total mass and is attached to the tip by a linear spring. Several viscous dampers were attached throughout the beam. The gap model simulates a loose connection between the beam and tip mass by a spring constant of zero within 13% of its maximum elastic deflection. The nonlinear material model used a bilinear connection spring whose coefficient was reduced by half once the spring deflection surpassed 33% of the maximum deflection.

Numerical simulations demonstrated the ability of the proposed time-domain modal identification approach to successfully identify linear mode approximations of nonlinear models and to characterize the nonlinearities by identifying the time-varying character of the modal parameters during the free-decay. Figure 4 shows frequency time histories for both nonlinear models. For a gap model in free-decay, the modal frequencies decreased as the am-

plitude of spring deflection decreased, which corresponds to a decrease in the average spring coefficient with decreasing amplitude. For a bilinear spring model, the modal frequencies were lower during the earlier time periods of the free-decay, and then increased throughout the free-decay due to an increase in the spring coefficient.

Random Data Processing

In situations where free-decay responses are corrupted by unmeasured random disturbances, the response data can be processed into cross-correlation functions that approximate free-decay responses of the structure. Consider a general n -DOF, linear time-invariant dynamic system, with equations of motion written in the form

$$M\ddot{x}(t+\tau) + C\dot{x}(t+\tau) + Kx(t+\tau) = f(t+\tau) \quad (4)$$

Premultiplying Eq. 4 by $x_i(t)$, a reference coordinate, integrating from 0 to T , and taking the limit as T tends to infinity:

$$\begin{aligned} & \lim_{T \rightarrow \infty} \frac{1}{T} \int_0^T x_i(t) M\ddot{x}(t+\tau) dt \\ & + \lim_{T \rightarrow \infty} \frac{1}{T} \int_0^T x_i(t) C\dot{x}(t+\tau) dt \\ & + \lim_{T \rightarrow \infty} \frac{1}{T} \int_0^T x_i(t) Kx(t+\tau) dt \\ & = \lim_{T \rightarrow \infty} \frac{1}{T} \int_0^T x_i(t) f(t+\tau) dt \end{aligned} \quad (5)$$

Differentiation and integration can be interchanged if the integrals in Eq. 5 converge uniformly:

$$\begin{aligned} & M \frac{d^2}{d\tau^2} \lim_{T \rightarrow \infty} \frac{1}{T} \int_0^T x_i(t) x(t+\tau) dt \\ & + C \frac{d}{d\tau} \lim_{T \rightarrow \infty} \frac{1}{T} \int_0^T x_i(t) x(t+\tau) dt \\ & + K \lim_{T \rightarrow \infty} \frac{1}{T} \int_0^T x_i(t) x(t+\tau) dt \\ & = \lim_{T \rightarrow \infty} \frac{1}{T} \int_0^T x_i(t) f(t+\tau) dt \end{aligned} \quad (6)$$

Equation 6 can be written in the condensed form

$$M\ddot{r}(\tau) + C\dot{r}(\tau) + Kr(\tau) = h(\tau) \quad (7)$$

where

$$\begin{aligned} r(\tau) & \equiv \lim_{T \rightarrow \infty} \frac{1}{T} \int_0^T x_i(t) x(t+\tau) dt \\ h(\tau) & \equiv \lim_{T \rightarrow \infty} \frac{1}{T} \int_0^T x_i(t) f(t+\tau) dt \end{aligned} \quad (8)$$

$r(\tau)$ and $h(\tau)$ are cross-correlation functions.¹⁴ If $f(\tau)$ is white noise, by definition

$$h(\tau) = 0 \quad (9)$$

Therefore, Eq. 7 becomes the homogeneous equations

$$M\ddot{r}(\tau) + C\dot{r}(\tau) + Kr(\tau) = 0 \quad (10)$$

Multiple data channels can be processed into auto/cross-correlation functions by selecting one channel as a reference, $x_i(t)$. The modal identification algorithm is then applied to $r(\tau)$. As shown in Eq. 10, these functions represent free-decay responses from initial conditions, $r(0)$, and the modal parameters are identical to those of the original data. In cases when $f(t+\tau)$ is not white noise and $h(\tau) \neq 0$, usable data can be obtained if the magnitude of responses due to $h(\tau)$ is sufficiently small compared to the responses of initial conditions, $r(0)$.

This random data processing approach together with the normal ERA method is theoretically equivalent to the eigensystem realization algorithm using data correlation (ERA/DC) method.¹⁵ It is noted that randomdec functions¹⁶ can be used in place of cross-correlation functions for the above random data processing.

Case Studies

The free-decay data processing strategies developed from the simple models were applied to three modal identification problems: (1) analytical simulations of the MIE, (2) modal test data from the Mini-Mast deployable truss, and (3) launch vehicle flight data. The first two studies were performed using both free-decay and forced response techniques for comparison, whereas the third study utilized the cross-correlation random data processing and sliding time window techniques. In all three cases, the ERA time-domain modal identification algorithm was employed and an extended modal amplitude coherence (EMAC) of greater than 80% was used to determine the identification of accurate modes. In addition, for the MIE simulations, it was required that identified modes differ from the analytical (true) model by a frequency error of less than 1%, damping factor error of less than 20%, and a modal assurance criterion (MAC) of greater than 90%.

MIE Simulation Case

The test time, data storage, and force measurement constraints lead to selection of a free-decay time-domain modal identification

Table 2 Mini-Mast modal identification results

Mode	Forced response				Free decay		
	Analytical freq. (Hz)	Freq. (Hz)	Damp. (%)	EMAC (%)	Freq. (Hz)	Damp. (%)	EMAC (%)
1st X Bend.	0.798	0.877	1.02	99.0	0.867	4.12	95.6
1st Y Bend.	0.799	0.890	2.56	97.9	0.878	2.73	97.9
1st Torsion	4.37	4.20	1.27	99.7	4.24	1.47	95.8
2nd X Bend.	6.11	6.14	1.87	99.5	6.14	4.38	88.1
2nd Y Bend.	6.16	6.19	1.14	99.3	6.22	1.80	96.6
2nd Torsion	21.6	22.9	0.647	94.0	23.0	1.01	92.3
3rd X Bend.	30.7	31.0	1.11	89.0	31.7	0.988	73.5
3rd Y Bend.	32.1	31.8	1.15	86.6	33.0	1.38	74.8
3rd Torsion	39.0	38.2	0.553	88.2	38.4	0.466	88.7
4th X Bend.	42.2	40.2	1.63	81.7	40.0	2.55	63.7
4th Y Bend.	44.9	43.4	0.639	93.3	43.7	0.286	72.8
4th Torsion	54.3	51.8	0.786	98.0	52.1	0.577	89.5
5th X Bend.	69.9	67.1	0.327	85.3	66.6	0.447	79.3
5th Y Bend.	70.2	67.3	0.319	85.3	67.1	0.244	71.3
5th Torsion	72.9	67.6	0.495	91.4	68.3	0.295	70.8

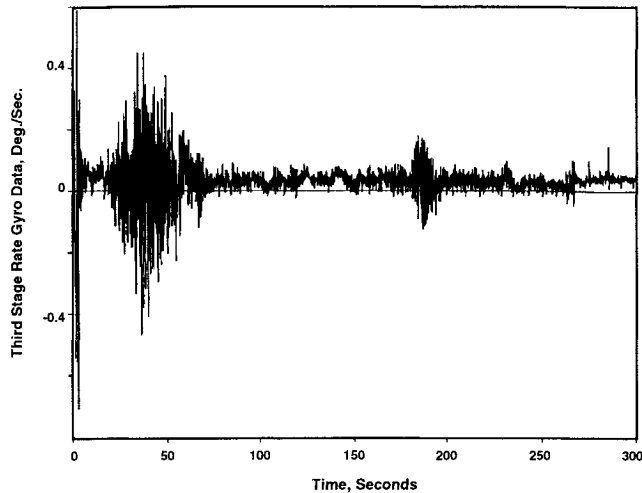


Fig. 7 Third-stage rate gyro data.

technique as a baseline for the MIE design.^{8,10} A potential threat to the performance of this modal identification method is large modal damping. This could cause the free-decay responses to decay too rapidly and affect the signal-to-noise (S/N) ratio. Thus, results from alternate forced response and free-decay techniques, assuming 2% modal damping, were compared to free-decay results with 1% modal damping. The forced response technique was expected to increase the S/N ratio by including data from the excitation periods as well as free decay periods in the modal analysis. Numerical simulations were performed using a 3834 DOF finite element model of the SSF assembly complete (AC) configuration (Fig. 5). The SSF is a large and complex structure that has a wide frequency range of interest and closely-spaced modes. Twenty important modes ranging from 0.12 to 1.2 Hz were preselected to evaluate the performance of each simulation case in identifying these target modes. A special random pulse excitation technique¹⁰ was applied at eight input points to excite modes of interest. It utilizes the ACS and reboost thrusters of the SSF and has the general form of burst random forcing functions.¹⁷

In the free-decay modal analysis case, four sets of forcing functions were sequentially applied to satisfy the multiple initial condition requirement for the separation of closely spaced modes. Acceleration responses were calculated at 159 measurement locations throughout the SSF for 150 s after each excitation of 50 s. Realistic data acquisition errors were added to the data, including bias error, scale factor error, electrical noise, digitization error, and sampling delay. For ERA analyses, the Hankel matrix was specially constructed to overcome the large data size and computational effort by selecting a larger number of rows than columns and emphasizing 20 critical channels while using all 159 channels to calculate complete mode shapes. In addition, the time-domain zooming technique with four frequency ranges was employed to identify the modes with high frequency aspect ratio.

In the forced response modal analysis case, the same random excitation for the free-decay case was used, but two changes were made to calculate FRFs. First, free-decay duration was extended to 155 s so that the structural responses decayed to 10% of their maximum values prior to the next excitation to minimize leakage errors.¹⁸ Second, the number of forcing function sets was increased to at least eight to avoid the singularity resulting from multipoint excitation.¹⁹ The same type of noise for the response data, but twice the level, was added to input data to account for inaccuracies in estimating input force from thruster chamber pressure data. In calculating FRFs, three different numbers of averages (8, 12, and 16) were taken using the data during both excitation and free-decay periods. Impulse response functions were generated from inverse Fourier transforms of FRFs and treated as free-decay data in the ERA analysis. The only change from the free-decay technique was that the size of the Hankel matrix had to be increased to incor-

porate the additional number of initial conditions while maintaining the length of the time window.

Modal identification results of the free-decay and forced response methods with and without simulated noise are presented in Table 1. As expected, increasing modal damping from 1 to 2% decreased performance of the free-decay method from all 20 modes identified with 1% damping to only 13 modes identified with 2% damping. The effect of noise on the free-decay results with 2% damping was minimal as 15 compared to 13 modes were identified when noise was removed from the data. As expected, the number of modes identified with the forced response method increased as the number of averages were increased from 8 to 16, but the effect of noise on the forced response method was much more pronounced than for the free-decay method. With 16 averages, the forced response method required more than four times the data acquisition time of the free-decay method, but only identified 8 modes compared to 13 with the free-decay method. Given the unique on-orbit testing constraints of the proposed MIE, the free-decay testing technique gave substantially better modal identification performance than an alternative forced response method.

Mini-Mast Truss Case

The Mini-Mast structure tested at the NASA Langley Research Center is a 20-m-high, deployable/retractable truss with triangular cross-section. This structure has been used for control-structure interaction research and has also had extensive modal testing.²⁰ The truss consists of 18 bays in a single-laced pattern that is repeated every other bay (Fig. 6). Its members are constructed of graphite/epoxy tubes and the joints are made of titanium. The longerons are hinged at both ends, while the diagonals are hinged at the mid-point and both ends. These hinges may introduce nonlinear behavior into the structure. The frequency range of interest was from 0.8 to 73 Hz and included the first five bending modes and the first five torsional modes.

Three shakers were located at bay 9 vertices and 25 burst random sequences of 32 s each were applied for a total test time of 800 s. Each burst random sequence was composed of 20 s of uncorrelated random excitation followed by a 12-s free-decay period. Displacement responses were measured at the vertices of four bays

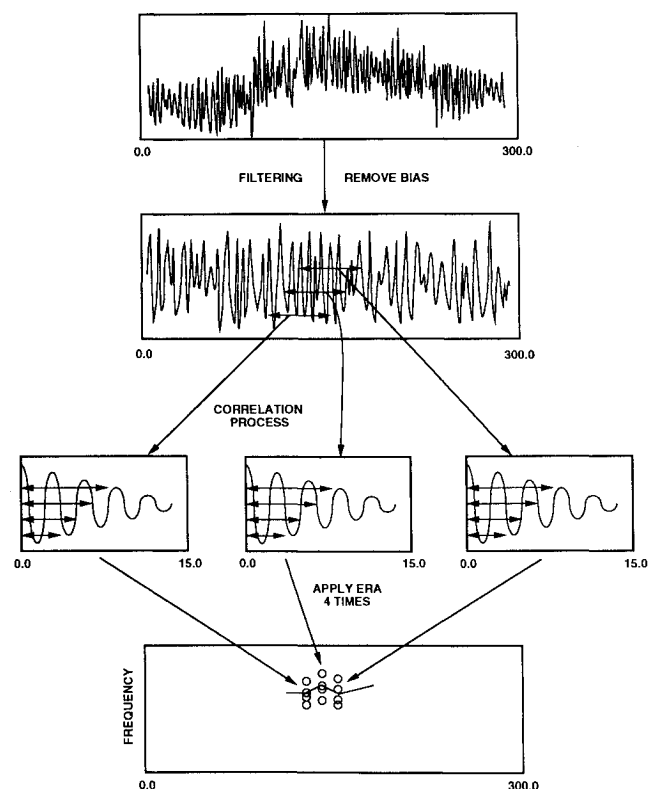


Fig. 8 Cross-correlation data reduction procedure.

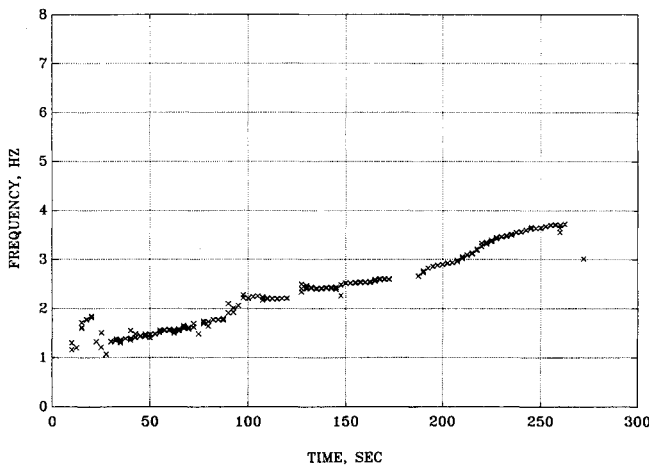


Fig. 9 Frequency time history plot.

(6, 10, 14, and 18) for a total of 12 measurements. The displacement sensors were located tangentially around the circumference of the cross section as shown in Fig. 6.

In order to evaluate the practicality of using limited free-decay data as proposed for the MIE, the free-decay modal identification technique using ERA was applied to only four sets of free-decay response data. In addition, the time-domain zooming technique was employed with six frequency ranges due to the high frequency aspect ratio of 91. The free-decay technique resulted in the identification of 8 of the 15 modes with EMAC values greater than 80% and 6 of the other 7 modes had EMAC values greater than 70% (Table 2). Damping values were 2–4% for the first two bending modes and were approximately 1% for the other modes, which generally agreed with the results from previous forced response modal identification.²⁰

The forced response method used 16 ensemble averages in FRF calculations. Impulse response functions were generated and treated as free-decay data in the ERA analysis. The three shakers used to excite the structure provided multiple initial conditions to separate the closely spaced modes. Modal identification results from the forced response analysis indicated that all 15 modes had been identified with EMAC values greater than 80% (Table 2). The identified frequencies and damping factors were very comparable between the results of the two techniques. The free-decay technique using time-domain zooming provided adequate modal identification results using only 4 of the 16 data sets used in the forced response modal identification.

Launch Vehicle Flight Data Case

The cross-correlation random data processing strategy developed in this study was applied to flight data of a launch vehicle in an attempt to identify modes excited by unmeasured random disturbance. Since the dynamic system is not stationary due to propellant mass loss, modal identification is possible only if response data over relatively short time intervals can be used. The first 300 s of third-stage rate gyro data (Fig. 7), spanning the liftoff, maximum dynamic pressure, and first-stage burnout events, was analyzed. Figure 8 illustrates the data processing strategy employed for this case study. The analysis was begun by prefiltering the response data using a band-pass FIR filter to eliminate aliasing and bias. A sliding time window technique was applied to characterize the system in a series of 15-s-long data windows at 2.5-s intervals throughout the entire data period. Autocorrelation functions were generated for these windows. It was assumed that the system remained sufficiently constant for a 15-s time span to allow modal identification.

The ERA was applied to each autocorrelation function four times by using a different data record length ranging from 1.0 to 2.3 s to evaluate repeatability of the modal parameter estimates. The closed-loop frequencies and damping factors for the first two structural bending modes were identified with EMAC values of at

least 80%. Figure 9 is a frequency time history plot for the first bending frequency where the absolute time was the midpoint for each 15-s window. Whereas the data processing technique employed in this study was able to identify a smooth trend for system frequencies, the identified damping factors had substantial data scatter, and no firm conclusions regarding system damping could be made. Several factors, including the nonstationary nature of the dynamic system, the data window length required to obtain the auto/cross-correlation functions, and the degree to which the random disturbances approximate white noise could affect the accuracy of the damping estimates. Further study is required to resolve these issues.

Conclusions

A free-decay time-domain modal identification technique has been developed to address major issues and solutions to on-orbit modal identification of large space structures. A data processing strategy was presented to generate equivalent free-decay responses from structural response data subject to unmeasured random input. The effectiveness of the free-decay technique was demonstrated in numerical simulations of the MIE, modal test data from the Mini-Mast deployable truss, and launch vehicle flight data. It was found that a free-decay time-domain modal identification technique can provide accurate modal parameters of large space structures and has been found to be more compatible with the limitations of on-orbit testing than conventional forced response techniques typically used in ground testing.

Acknowledgments

The research summarized in this paper was conducted under Contract NAS9-18200 with the NASA Johnson Space Center and with technical management provided by the NASA Langley Research Center.

References

- ¹Allemang, R. J., "Multiple-Input Experimental Modal Analysis—A Survey," *International Journal of Analytical and Experimental Modal Analysis*, Vol. 1, No. 1, 1986, pp. 37–44.
- ²Carbon, G. D., "Ground Vibration Testing at Boeing," *Sound and Vibration*, Vol. 18, No. 6, 1984, pp. 16–20.
- ³Denman, E. D., Hasselman, T., Sun, C. T., Juang, J. N., Junkins, J., Udawadia, F., Venkayya, V., and Kamat, M., "Identification of Large Space Structures," ASCE Report No. AFRPL TR-86-054, New York, Sept. 1986.
- ⁴Kim, H. M., "System Identification for Large Space Structures," Ph.D. Dissertation, Univ. of Texas, Austin, TX, Dec. 1988.
- ⁵Pappa, R. S., "Identification Challenges for Large Space Structures," *Sound and Vibration*, Vol. 24, No. 4, 1990, pp. 16–21.
- ⁶Ljung, L., *System Identification: Theory for the User*, Prentice-Hall, Englewood Cliffs, NJ, 1987, p. 73.
- ⁷Juang, J. N., Phan, M., Horta, L. G., and Longman, R. W., "Identification of Observer/Kalman Filter Markov Parameters: Theory and Experiments," *Proceedings of the AIAA Guidance, Navigation, and Control Conference* (New Orleans, LA), AIAA, Washington, DC, 1991, pp. 1195–1207.
- ⁸Kim, H. M., and Doiron, H. H., "Modal Identification Experiment Design for Large Space Structures," *Proceedings of the AIAA 32nd Structures, Structural Dynamics, and Materials Conference* (Baltimore, MD), AIAA, Washington, DC, 1991, pp. 2968–2976.
- ⁹Brown, D., Carbon, G., and Ramsey, K., "Survey of Excitation Techniques Applicable to the Testing of Automotive Structures," *Society of Automotive Engineers Technical Paper Series*, Paper 770029, Society of Automotive Engineers, Warrendale, PA, 1977.
- ¹⁰Kim, H. M., and Doiron, H. H., "On-Orbit Modal Identification of Large Space Structures," *Sound and Vibration*, Vol. 26, No. 6, 1992, pp. 24–30.
- ¹¹Pappa, R. S., Shenk, A., Niedbal, N., and Klusowski, E., "Comparison of Two Dissimilar Model Identification Techniques," *Proceedings of the International Forum on Aeroelasticity and Structural Dynamics* (Aachen, Germany), DGLR, Bonn, Germany, 1991, pp. 195–203.
- ¹²Juang, J. N., and Pappa, R. S., "An Eigensystem Realization Algorithm for Modal Parameter Identification and Model Reduction," *Journal of Guidance, Control, and Dynamics*, Vol. 8, No. 5, 1985, pp. 620–627.
- ¹³Pappa, R. S., and Juang, J. N., "Some Experiences with the Eigensystem Realization Algorithm," *Sound and Vibration*, Vol. 22, No. 1, 1988, pp. 30–34.

¹⁴Bendat, J. S., and Piersol, A. G., *Random Data: Analysis and Measurement Procedures*, Wiley, New York, 1971, pp. 28–31.

¹⁵Juang, J. N., Cooper, J. E., and Wright, J. R., "An Eigensystem Realization Algorithm Using Data Correlation (ERA/DC) for Modal Parameter Identification," *Journal of Control Theory and Advanced Technology*, Vol. 4, No. 1, 1988, pp. 5–14.

¹⁶Reed, R. E., "Analytical Aspects of Randomdec Analysis," *Proceedings of the AIAA 20th Structures, Structural Dynamics, and Materials Conference* (St. Louis, MO), AIAA, New York, 1979.

¹⁷Olsen, N., "Burst Random Excitation," *Sound and Vibration*, Vol. 17,

No. 11, 1983, pp. 20–23.

¹⁸Taber, R. C., Vold, H., Brown, D. L., and Rocklin, G. T., "Exponential Window for Burst Random Excitation," *Proceedings of the Third International Modal Analysis Conference* (Orlando, FL), Society for Experimental Mechanics, Bethel, CT, 1985, pp. 989–995.

¹⁹Ewins, D. J., *Modal Testing: Theory and Practice*, Wiley, New York, 1984, p. 152.

²⁰Pappa, R. S., Schenk, A., and Noll, C., "Eigensystem Realization Algorithm Modal Identification Experience with Mini-Mast," NASA TM-4307, Feb. 1992.